Proceedings of the XXIII Conference on Applied Crystallography, Krynica Zdrój, Poland, September 20–24, 2015

Structure Characterization of Biomedical Ti–Mo–Sn Alloy Prepared by Mechanical Alloying Method

G. Dercz*, I. Matuła, M. Zubko and A. Liberska
Institute of Materials Science, University of Silesia, 75 Pułku Piechoty 1A, 41-500 Chorzów, Poland

The study presents the results of the influence of high energy milling on the structure of the new Ti–15Mo–5Sn [wt%] alloy for biomedical applications. During testing the powders were milled for the following milling times: 5, 15, 30, and 45 h. The milled powders were characterized by X-ray diffraction, scanning and transmission electron microscopy methods. Observation of the powder morphology after various stages of milling leads to the conclusion that with the increase of the milling time the size of the powder particles as well as the degree of aggregation change. However, a clear tendency of particles reduction at every stage of the mechanical alloying process is clearly observed. The X-ray diffraction results confirmed the presence of the α and β phases, and molybdenum. It has been found that the reflections from the Sn phase disappeared after five hours of milling, suggesting that the Sn and Ti alloying took place, leading to the creation of a titanium-based solid solution. After 30 and 45 h of mechanical alloying the formation of the β-Ti phase, the final share of which is 46(4) wt%, was observed. Furthermore, it was found that a diffraction line broadening with the increase of the milling time results from reduction of the crystallite size and an increase in the lattice distortion. The maximum level of the reduction of the crystallite size was obtained after 45 h of milling. The maximum degree of the unit cells reduction for all phases present in the powder that was being milled was also observed for this milling time.

DOI: 10.12693/APhysPolA.130.1029
PACS/topics: 81.05.Bx, 87.85.J–, 81.20.Ev, 61.05.cp, 68.37.Og

1. Introduction

The interest in titanium-based materials is still increasing due to their high biocompatibility, corrosion resistance, light weight, good mechanical properties, and low elastic module [1]. Titanium-based alloys also exhibit another interesting property — shape memory effect (SME). The phenomenon of reverse martensitic transformation can be found in NiTi alloys [2, 3]. However, the Ni-hypersensitivity and toxicity of Ni have been observed in Ti–Ni alloys [4, 5]. Thus, the development of biocompatible Ni-free shape memory alloys (SMAs) is strongly required. Recently, many biocompatible Ti-based alloys with shape memory effect and superelastic (SE) such as Ti–Mo–base have been studied by many researchers. The β-Ti alloys reveal a martensitic transformation from β (disordered bcc) to two metastable martensite structures, either hexagonal martensite (α') or orthorhombic martensite (α''), by quenching [6]. Thus, molybdenum is an effective β stabilizer. Previous studies have also shown excellent mechanical compatibility and good cytocompatibility of Ti alloys containing Mo [7, 8]. Tin is a neutral element, hence it does not stabilize the α and β phases. In contrast, several authors observed the influence of Sn on the temperature of the martensitic transformation and that it inhibits the formation of the metastable phase ω. Thus, Mo and Sn are desirable as an alloying element for the development of Ti-based biomaterials [7, 9].

Conventionally, these alloys are prepared by melting techniques, in arc furnace, followed by specific thermomechanical treatments for homogenization and ageing and additional mechanical machining to get the needed shape. All these processes are done under vacuum or inert atmosphere because oxidation damages drastically the properties [6–8]. Recently there has been significant interest in adopting new non-conventional techniques such as powder metallurgy (PM) based on a high-energy ball-milling process. The mechanical alloying (MA) is a solid-state powder metallurgical process and is capable of processing Ti alloys with homogeneous microstructures and improved mechanical properties than the conventional powder metallurgy or casting techniques [10, 11]. Over the past few years, mechanical alloying has shown great potential in synthesizing a wide variety of nanocrystalline, supersaturated solid solutions and amorphous phase with unique characteristics [12–14].

In the present study, a biomedical Ti–15Mo–5Sn [wt%] alloy was fabricated from elemental powders via the MA process for different ball-milling times.

2. Experimental details

The main objective is an attempt at using mechanical synthesis of the Ti, Mo, and Sn powders to obtain the Ti–15Mo–5Sn alloy. As the initial material, the following commercial powders were used: Ti (Atlantic Equipment Engineers (AEE), purity 99.7%, particle size $\leq$20 μm), Mo (AEE, purity 99.7%, particle size $\leq$2 μm) and Sn (Sigma Aldrich, purity 99.9%, $\leq$44 μm). Weighted amounts with the composition corresponding to Ti–15Mo–5Sn alloy [wt%] were put under the high

*corresponding author; e-mail: grzegorz.dercz@us.edu.pl

energy milling process in the planetary ball mill PULVERISETTE 7 premium line by Fritch. Containers and balls (with the diameter of 10 mm) made of tempered steel were used, and the weight ratio of the balls to the weight of the powder was 10:1. Ball milling was carried out at the rotational speed of 400 rpm and was the same for all tests. To prevent the powder from oxidation to the minimum, the process was carried out in argon protective-gas atmosphere.

The most important variable of the process of mechanical synthesis is the milling time which is responsible for the final composition of the powders, the microstructure and the mechanical properties of a certain alloy. During testing, the powders were milled for the following times: 5, 15, 30, and 45 h.

The crystalline structure and phase content of the obtained milled and sintered materials were tested by X-ray diffraction. The refinement of the X-ray diffraction pattern was carried out using the Rietveld whole X-ray profile fitting technique with the DBWS 9807a program [15]. The profile function used to adjust the calculated diffractograms to the observed ones was the pseudo-Voigt one [16, 17]. The weight fraction of each component was determined based on the optimized scale factors with the use of the relation proposed by Hill and Howard, and Dercz et al. [18, 19]. The size of the crystallites and the lattice distortion of the α and β phases were measured by the Willamson–Hall method [20].

The morphology of the powder was tested using the scanning microscope JEOL JSM 6480 with the accelerating voltage of 20 kV. Chemical analysis was performed using the EDS detector manufactured by IXRF using the standard calibration method.

The size of the crystallites was verified using the transmission electron microscope JEM 3010, operated at the accelerating voltage of 300 kV. The material that was tested was placed on copper grid covered by thin layer of carbon.

3. Results and discussion

The morphology of Ti–15Mo–5Sn powders after various milling stages are presented in Fig. 1. The microphotographs clearly show progressive changes in the morphology of the particles at different milling stages. During milling in a ball mill for 5 h, a significant advantage of cold welding can be observed. Further milling results in the formation of agglomerates. Microphotographs of the powders milled in a ball mill for 15 h showed the appearance of fine particles and many larger agglomerates. The formation of the agglomerated particles is due to the domination of cold welding over fracturing. The structure of the samples shows a breakdown of the grain into smaller particles. The formation of fine particles and smaller variation in the composition between the particles for longer milling times results in a higher degree of homogeneity. At the stage of milling for 30 h plastic powders are agglomerated into larger particles and further deformation of the charge can be observed. For a longer ball-milling time, the particles gradually formed larger agglomerates. During milling up to 45 h, the observed microstructure is formed by fracturing and re-welding of the flattened particles. At this stage, the particles showed irregular sizes — fragmented grains and larger agglomerates could be observed.

Figure 2 shows a summary of the diffraction patterns of the material after mechanical synthesis, depending on the milling time of initial powders. A change of the profile line on individual diffraction patterns is clearly visible. For the sample milled for 5 h, no diffraction reflections coming from Sn were observed. It seems that it was the plastic nature of the tin that caused the powder to have been incorporated into the titanium unit cell.

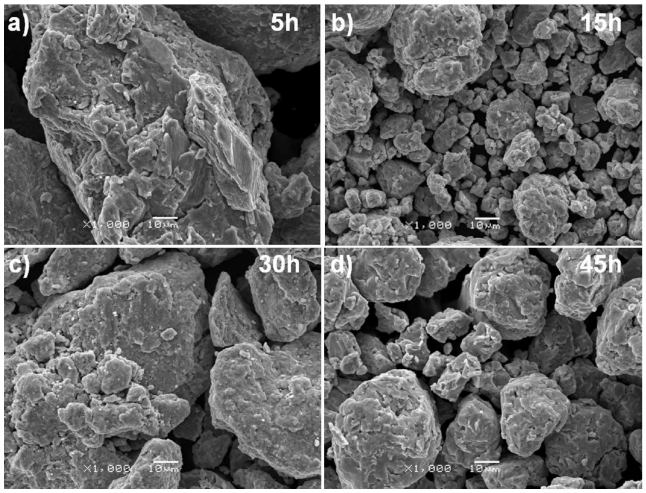

Fig. 1. SEM images of the powder after: (a) 5 h, (b) 15 h, (c) 30 h, and (d) 45 h of milling process.

The analysis showed that only two alpha phases — titanium and molybdenum — are present in the material, the crystallites of which have the size of 36(2) nm and 43(3) nm. The main difference on the diffraction patterns can be seen as early as after 15 h of milling. At this stage, broadening of the diffraction lines can be observed, which is associated with the beginning of the process of reducing the size of crystallites and an increase of lattice strain (Table I). The estimated size of the crystallites for this milling stage is 8(1) nm and 27(2) nm for the α and Mo phases, respectively. The observed $\langle \Delta a/a \rangle$ lattice strain value indicates a growth for the alpha phase ($1.31 \times 10^{-3}\%$) with a slight lattice strain ($3.31 \times 10^{-4}\%$) for the hard Mo. The extension of the diffraction lines after 30 and 45 h clearly points to the increase in the crystallite size, with the final value of 7(1) nm for the alpha phase and 21(2) nm for molybdenum. A much larger size of the molybdenum crystallites in relation to other phases is due to its high hardness and resistance to fragmentation, which resulted in the fact that the synthesis did not proceed in full. For the mixture after 30 h of milling the diffraction patterns showed clear lines in-

dicating the beginning of the titanium beta phase. The contribution in the alloy structure of titanium beta phase reaches 46% after 45 h of milling. The reflections from the beta phase are relatively wide due to the nanocrystalline size 6(1) nm and a significant share (1.16×10^{-3}%) of the second type $\langle\Delta a/a\rangle$ deformations. A detailed analysis of the milling products did not show any unwanted phases originating from the material in the container or the milling balls to be formed.

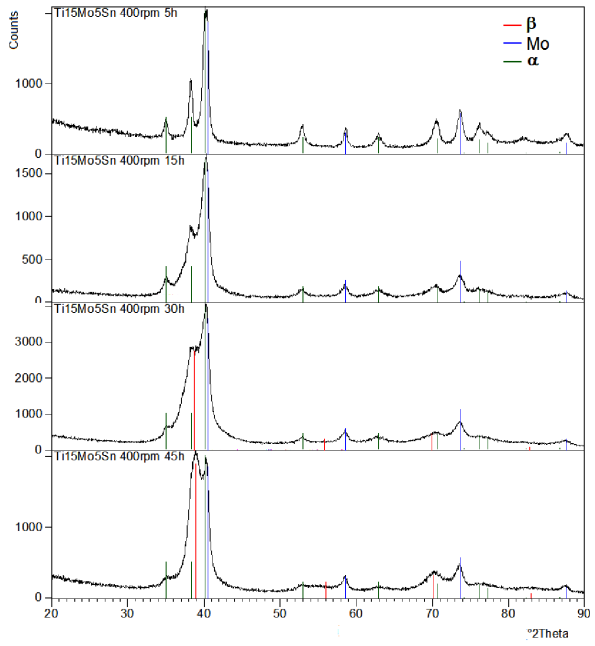

Fig. 2. X-ray diffraction patterns of the powder after 5, 15, 30, and 45 h of the milling process.

TABLE I

Changes of lattice distortion ($\langle\Delta a/a\rangle$ [%] and average crystallite size D [mm] of the α, β and Mo phases of the milled powders.

Phase	Parameters	Milling time [h]			
		5	15	30	45
α	D	36(2)	8(1)	9(1)	7(1)
	$\langle\Delta a/a\rangle\times10^3$	2.04	1.31	1.16	2.43
β	D	—	—	7(2)	6(2)
	$\langle\Delta a/a\rangle\times10^3$	—	—	3.12	1.16
Mo	D	43(3)	27(2)	23(2)	21(2)
	$\langle\Delta a/a\rangle\times10^4$	7.13	3.31	3.31	3.62

The analysis of the diffraction patters obtained using the Rietveld method showed that when the milling time increases, the lattice parameters for all tested samples become reduced (Table II). In comparison to the ICDD data it has been found that high energy milling has the smallest, but successive effect on the reduction of the size of the unit cell of molybdenum (0.3140(1) nm) due to its considerable hardness. Whereas for the remaining phases, i.e. α and β, the tendency of the lattice parameter compression is significant. Thus, the β phase, due to its plastic nature and the presence of its stabilizer (Mo), reaches the a_0 reduced by 0.04 nm after 45 h of milling. A similar class of cell contraction was discovered for the a_0 parameter of the α phase; and for the c_0 parameter these changes are smaller, which results from shift systems for the phases of the hexagonal system.

TABLE II

Lattice parameters [nm] of α, β and Mo phases of the milled powders

Phase	Lattice param.	ICDD*	Milling time [h]			
			5	15	30	45
α	a_0	0.2970	0.2948(6)	0.2938(6)	0.2936(6)	0.2936(2)
	c_0	0.4720	0.4693(1)	0.4699(2)	0.4697(2)	0.4702(3)
β	a_0	0.3307	—	—	0.3270(2)	0.3268(2)
Mo	a_0	0.3147	0.3148(3)	0.3147(1)	0.3142(1)	0.3140(1)

*International Centre for Diffraction Data®

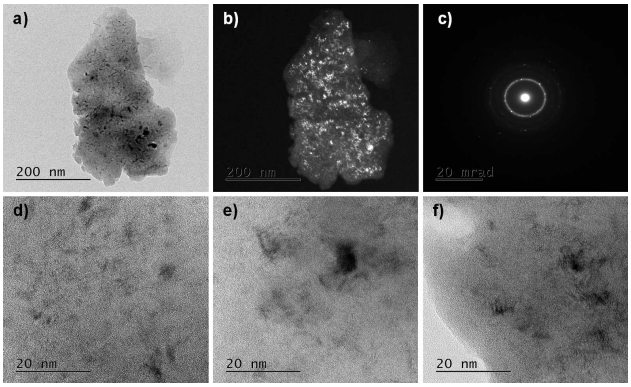

Fig. 3. TEM analysis of α and β phases after 45 h milling process presents a bright-field (a,d–f), a dark-field (b), and an SAD pattern (c).

The effect of the long-term high-energy milling on the nanocrystallization of the powder after 45 h of milling was confirmed using a transmission electron microscope. The analysis of the obtained images in a bright and dark fields and of the diffraction image proved the nanocrystalline nature of the material after milling (Fig. 3). Sample images of the powder after 45 h of milling obtained in bright and dark field show that a single particle of the powder is composed of many smaller crystallites with different orientations (Fig. 3).

4. Conclusion

1. The effect of the high-energy milling time of the substrates on the structure and phase composition of the Ti–15Mo–5Sn [wt%] alloy was observed.
2. XRD and TEM studies point to the formation of β phase during high-energy ball milling of the precursor mixture of Ti, Mo and Sn.

3. X-ray and electron microscopy studies are a proof of the presence of the α, β, and Mo as nanocrystalline phases. Moreover, the agglomeration of powder particles is observed.

Acknowledgments

This work was supported by the Polish National Science Centre (NCN) under the research project no. UMO-2011/03/D/ST8/04884.

References

[1] M. Long, H.J. Rack, *Biomaterials* **19**, 1621 (1998).

[2] S. Miyazaki, K. Otsuka, *ISIJ Int.* **29**, 353 (1989).

[3] H. Morawiec, D. Stróż, T. Goryczka, D. Chrobak, *Scr. Mater.* **35**, 485 (1996).

[4] S. Shabalovskaya, in: *Proc. First Int. Conf. on Shape Memory and Superelastic Technologies*, Eds.: A.R. Pelton, D. Hodgson, T.W. Duerig, Asilomar Conference Center, Pacific Grove (CA) 1994, p. 209.

[5] Y. Cheng, Y.F. Zheng, *Surf. Coat. Technol.* **201**, 4909 (2007).

[6] J.I. Kim, H.Y. Kim, T. Inamura, H. Hosoda, S. Miyazaki, *Mater. Sci. Eng. A* **403**, 334 (2005).

[7] F.F. Cardoso, P.L. Ferrandini, E.S. Lopes, A. Cremasco, R. Caram, *J. Mech. Behav. Biomed. Mater.* **32**, 31 (2014).

[8] N. Oliveira, G. Aleixo, R. Caram, A.C. Guastaldi, *Corros. Sci.* **50**, 938 (2007).

[9] T. Maeshimaa, S. Ushimaru, K. Yamauchi, M. Nishida, *Mater. Sci. Eng. A* **438-440**, 844 (2006).

[10] H.C. Hsu, S.C. Wu, S.K. Hsu, T.Y. Chang, W.F. Ho, *J. Alloys Comp.* **582**, 793 (2014).

[11] A. Nouri, P.D. Hodgson, C. Wen, *Mater. Sci. Eng. C* **31**, 921 (2011).

[12] C. Suryanarayana, *Prog. Mater. Sci.* **46**, 1 (2001).

[13] G. Dercz, B. Formanek, K. Prusik, L. Pajak, *J. Mater. Process. Tech.* **162**, 15 (2005).

[14] G. Dercz, J. Dercz, K. Prusik, A. Hanc, R. Babilas, L. Pajak, J. Ilczuk, *Archiv. Metall. Mater.* **54**, 741 (2009).

[15] H.M. Rietveld, *J. Appl. Crystallogr.* **3**, 65 (1969).

[16] D.B. Wiles, R.A. Young, *J. Appl. Cryst.* **14**, 149 (1981).

[17] *The Rietveld Method*, Ed. R.A. Young, Oxford Univ. Press, New York 1993.

[18] R.J. Hill, C.J. Howard, *J. Appl. Crystallogr.* **20**, 467 (1987).

[19] G. Dercz, D. Oleszak, K. Prusik, L. Pająk, *Rev. Adv. Mater. Sci.* **8**, 764 (2008).

[20] G.K. Williamson, W.H. Hall, *Acta Metall.* **1**, 22 (1953).